For submission to Water Research as a **Research Paper**

Application of Fluorescence Spectroscopy Using a Novel Fluoroionophore for Quantification of Zinc in Urban Runoff

Akira Hafuka[a], Hiroaki Yoshikawa[a], Koji Yamada[b], Tsuyoshi Kato[c], Masahiro Takahashi[a], Satoshi Okabe[a], and Hisashi Satoh[a,*]

[a] Division of Environmental Engineering, Graduate School of Engineering, Hokkaido University, North-13, West-8, Sapporo 060-8628, Japan

[b] Division of Environmental Materials Science, Graduate School of Environmental Science, Hokkaido University, North-10, West-5, Sapporo 060-0810, Japan

[c] Department of Computer Science, Graduate School of Engineering, Gunma University, 1-5-1 Tenjin-cho, Kiryu 376-8515, Japan

E-mail:

Akira Hafuka: hafuka@eng.hokudai.ac.jp

Hiroaki Yoshikawa: spg377m9@gmail.com

Koji Yamada: yamada@ees.hokudai.ac.jp

Tsuyoshi Kato: katotsu@cs.gunma-u.ac.jp

Masahiro Takahashi: m-takaha@eng.hokudai.ac.jp

Satoshi Okabe: sokabe@eng.hokudai.ac.jp

Hisashi Satoh: qsatoh@eng.hokudai.ac.jp

*Corresponding author

Hisashi Satoh, Division of Environmental Engineering, Graduate School of Engineering, Hokkaido University, North-13, West-8, Sapporo 060-8628, Japan.

Tel: +81-(0)11-706-6277 Fax: +81-(0)11-706-6277 E-mail: qsatoh@eng.hokudai.ac.jp

ABSTRACT

Fluorescence spectroscopy has great potential for on-site and real-time monitoring of pollutants in aquatic environments; however, its application to environmental aquatic samples has been extremely limited. In this study, a novel fluoroionophore based on a BODIPY-terpyridine conjugate was developed and applied to determine Zn concentrations in urban runoff. The fluoroionophore selectively bound to Zn^{2+} in water, which led to an instant red-shift of the fluorescence peak of the fluoroionophore from 539 nm to 567 nm that could be seen by the naked eye. Zn concentrations could be quantified using the ratio of fluorescence intensities, and the detection limit was 9 μg/L, which is sufficiently low for environmental aquatic samples. To demonstrate applicability of the method to environmental samples, we measured Zn concentrations in urban runoff samples with a complex matrix (~60 mg/L dissolved organic carbon and ~20 mS/cm electrical conductivity). The total and dissolved fractions of Zn in the samples could be determined by fluorescence spectroscopy and its relative error was estimated to be less than 30% by inductively coupled plasma-atomic emission spectroscopy analysis. The proposed method is rapid and easy-to-use with simple pretreatment for Zn determination in environmental aquatic samples with complex matrices.

Keywords: Fluorescence spectroscopy; Zinc; Fluoroionophore; Urban runoff; Spearman's rank correlation analysis

1. Introduction

Rapid urbanization is a global phenomenon that is often associated with adverse environmental effects. In urban environments, contaminants from vehicles and buildings accumulate on road surfaces until they are washed off into local aquatic systems by rainfall events, where they compromise water resources. In such areas, reuse and recycling of water may be needed to enable sustainable water management (Bischel et al., 2012). Accordingly, on-site and real-time monitoring technologies are necessary to measure contaminant levels and ensure water quality. Heavy metals are one of the most hazardous pollutants in aquatic environments. Zn is a common metal that is widely used for industrial applications in chemical and alloyed products, fabricated metal products, and paper products (Naito et al., 2010). In recent years, Zn has received increased attention owing to concerns about its toxic effects on aquatic life. In Japan, the environmental quality standard for Zn is 30 μg/L in freshwater (Japanese Ministry of Environment, Environmental quality standards for water pollution). Urban runoff is considered to be one of the main sources of Zn found in surface water (Naito et al., 2010).

Currently, the most common analytical methods for heavy metals including Zn are atomic absorption spectrometry (AAS) and inductively coupled plasma (ICP) spectroscopy (Adeloju et al., 2009; Majedi et al., 2012). Although these methods are precise, they are expensive and often require complex sample preparation. In addition,

70 they are not applicable to continuous on-site monitoring and measure only the total
71 concentration of heavy metals. Simple analytical methods such as colorimetric or
72 electrochemical techniques have recently been developed for rapid detection of heavy
73 metals (Yan et al., 2012; Gong et al., 2010). Among these methods, fluorescence
74 spectroscopy has attracted a great deal of attention from environmental engineers owing
75 to its high sensitivity, simplicity, and versatile instrumentation (Lakowicz, 2006).
76 Although fluorescence excitation-emission matrix (EEM) measurements have been
77 employed to monitor water quality, their application to detection of trace amounts of
78 contaminants is limited to monitoring of dissolved organic matter, such as humic-like
79 and protein-like matters (Henderson et al., 2009). In contrast, fluoroionophores are
80 usually used for detection of heavy metals in biochemistry (Domaille et al., 2008). A
81 fluoroionophore is an organic molecular indicator that exhibits quantifiable changes in
82 fluorescence spectra upon binding a particular guest ion. The design and development of
83 novel fluoroionophores remains an active area of research, and various fluoroionophores
84 for heavy metal ions have been reported (Li et al., 2009; Weng et al., 2009; Li et al.,
85 2008). However, their application for environmental use has been extremely limited.
86 Here, we developed a fluoroionophore for determination of total and dissolved Zn
87 concentrations in urban runoff by fluorescence spectroscopy. The photo-physical
88 properties of the fluoroionophore were also reported. This approach enabled screening of
89 the Zn levels with no complicated pretreatment processes.
90

91 **2. Materials and methods**

92 2.1 Urban runoff sampling and testing

93 Urban runoff samples were collected from heavy traffic areas in four cities in
94 March and April 2012 during rainfall events: Gifu (+35° 26' 54.88", +136° 44' 28.15"),
95 East-Hiroshima (+34° 24' 4.40", +132° 43' 1.43"), Osaka (+34° 43' 50.46", +135° 32'
96 48.40"), and Tsukuba (+36° 3' 38.05", +140° 7' 11.92"). Samples were preserved in
97 500-mL polypropylene bottles at 4°C. All polypropylene bottles and glassware were
98 previously soaked for at least 24 h in 2 M HNO_3 and then rinsed thoroughly with Milli-Q
99 water. Following filtration through a 0.45-μm-pore-size membrane, the dissolved organic
100 carbon (DOC) was measured by total organic carbon analyzer (TOC-VCSH;
101 SHIMADZU Corporation, Kyoto, Japan). pH and electrical conductivity (EC) were
102 measured by pH meter (D-54; HORIBA, Ltd., Kyoto, Japan) and EC meter (ES-51;
103 HORIBA, Ltd., Kyoto, Japan). Additionally, 0.45-μm-pore-size cellulose ester
104 membrane was used to fractionate dissolved metals. Nitric acid digestion was performed
105 before metal analysis by ICP/atomic emission spectrometry (AES) [ICPE-9000;
106 SHIMADZU Corporation, Kyoto, Japan]. To accomplish this, each urban runoff sample
107 (9 mL) and concentrated HNO_3 (1 mL) were added into 10-mL test tubes and samples
108 were then digested on an aluminum heating block with watch glasses at 95°C for 2.5 h
109 and cooled to room temperature. Following filtration through a 0.45-μm-pore-size
110 membrane, the concentrations of Zn, Al, Cd, Cr, Cu, Fe, Mn, Ni, Pb, and Sb were
111 determined by ICP/AES. These metals were selected because they are generated by motor
112 vehicles (Mahbub et al., 2010). All reported data are the averages of at least three
113 replicates.
114
115 2.2 Fluorescence spectroscopic measurement

The fluoroionophore designed in our laboratory was synthesized according to a previously described method (Hafuka et al., 2013). Milli-Q water (18.25 MΩcm) was used to prepare all aqueous solutions. Stock solutions of fluoroionophore (40 μM) were prepared by dissolving the fluoroionophore in acetonitrile, while stock solutions of metal ions for calibration were prepared by dissolving appropriate amounts of perchlorate or chloride salts in Tris-HCl buffer. For analysis of total zinc (T-Zn) in actual urban runoff samples, the samples were acidified with HCl to dissolve the complexed Zn. HNO_3 was not used in this experiment because Tris-HCl buffer was appropriate for our fluoroionophore in terms of fluorescence intensity. Each urban runoff sample (36 mL) and 1 M HCl (2 mL) were added into 50-mL beakers and vigorously mixed at room temperature for 15 min. After mixing, each sample solution was filtered through a 0.45-μm-pore-size membrane to remove suspended solids, after which 1 M NaOH solution was added to neutralize the pH. To measure the dissolved Zn (D-Zn), samples were filtered through a 0.45-μm-pore-size membrane as the sole pretreatment. All spectroscopic measurements were carried out in an aqueous acetonitrile solution (CH_3CN/H_2O=1/1, v/v). Test solutions were prepared by adding an appropriate aliquot of the fluoroionophore stock solution into a volumetric flask, followed by 4.5 mL of the pretreated urban runoff samples and 0.5 mL of a Tris-HCl buffer adjusted to pH 7.0, and finally by diluting the solution to 10 mL with acetonitrile. Quartz cells with a cross section of 1 cm × 1 cm were used for fluorescence and absorption spectroscopic measurements (FP-6600 and V-630; JASCO Corporation, Tokyo, Japan). The excitation and fluorescence slit widths were 5.0 and 6.0 nm, respectively. The detection limit (LOD, 3σ/slope) and quantification limit (LOQ, 10σ/slope) for Zn^{2+} were determined based on

the standard deviation (σ) of 11 blank solutions (Han et al., 2010). As a natural organic matter (NOM) standard, IHSS Suwannee River NOM (RO isolation, 1R101N) was used. The NOM was dissolved in Tris-HCl buffer (pH 7) and the solution was filtered through a 0.45-μm-pore-size membrane. The DOC concentration was obtained by analyzing the NOM solution and the Tris-HCl buffer by using total organic carbon analyzer. The NOM solution was used for fluorescence titration of the fluoroionophore with and without Zn^{2+} solution (10 μM). The fluorescence quantum yields were obtained by comparing the area under the corrected fluorescence spectrum of the test sample with that of a solution of Rhodamine 6G in H_2O, which has a reported quantum yield (Φ_R) of 0.76 (Olmsted, 1979). The quantum yields of fluorescence (Φ_S) were obtained from multiple measurements (N = 3) using the following equation:

$$\Phi_S = \Phi_R \times S_S/S_R \times A_R/A_S \times (\eta_S/\eta_R)^2,$$

where Φ is the quantum yield, S is the integrated area of the corresponding fluorescence spectrum, A is the absorbance at the excitation wavelength, η is the refractive index of the solvent used, and S and R refer to the sample and the reference fluorophore, respectively. All reported data are the averages of at least three replicates.

2.3 Data analysis

To investigate the interference effects on fluorescence measurements of Zn in urban runoff samples, Spearman rank correlation coefficients (r_s) for metals, protons, DOC, and EC were computed toward the absolute difference between a Zn concentration determined by ICP and that of fluoroionophore. The procedure for computing the Spearman rank correlation coefficient is described as follows (Rosner, 2011). Detailed

procedure of the data analysis is in the supporting information section.

3. Results and discussion

3.1 Fluorescence titration of the fluoroionophore with Zn^{2+}

The fluoroionophore consisted of a 4,4-difluoro-4-bora-3a,4a-diaza-s-indacene (BODIPY) fluorophore and a 2,2′:6′,2′′-terpyridine receptor. BODIPY fluorophores possess many valuable characteristics, such as sharp and intense absorption and fluorescence bands, high fluorescence quantum yields, high molar absorption coefficients, and good photo-chemical stability (Loudet et al., 2007). The terpyridine receptor is a metal ion ligand known to bind to Zn^{2+} with a high binding constant (Piao et al., 2009). Figure 1-(a) shows the absorption and the fluorescence spectra of the fluoroionophore. The fluoroionophore exhibited a strong absorption band around 516 nm with a large molar absorption coefficient ($\varepsilon = 7.5 \times 10^4$ $Lmol^{-1}cm^{-1}$). The fluoroionophore also showed a sharp fluorescence peak at 539 nm (half bandwidth was 26 nm) with a shoulder around 580 nm, which is typical of BODIPY fluorophores (Karolin et al., 1994). The fluorescence quantum yield was high ($\Phi = 0.73$). Upon addition of excess Zn^{2+} (100 eq.), both the absorption and the fluorescence bands were red-shifted (Figure 1-(a)) from 516 nm to 533 nm (17 nm) and from 539 nm to 567 nm (28 nm), respectively, with a decrease in the intensity. The molar absorption coefficient decreased to 5.4×10^4 upon complexation with Zn^{2+}. The fluoroionophore still exhibited high fluorescence quantum yield (0.49), and changes in fluorescence and absorption color were easily distinguishable by the naked eye (Figure 1-(b)). The red-shifted spectra of the fluoroionophore upon complexation could be explained by enhanced intramolecular charge transfer (ICT) between the 1-alkyloxy

BODIPY fluorophore and the terpyridine ionophore moieties (Hong et al., 2011). Because of the d^{10} electron configuration of Zn^{2+} ions, metal-to-ligand charge-transfer processes do not occur in this system (Liang et al., 2012). Terpyridine might be slightly electron-withdrawing when compared with the BODIPY with the electron-donating 1-alkyloxy group. The electron-withdrawing property of terpyridine is enhanced upon complexation with Zn^{2+}, which promotes the ICT process from the BODIPY core to the terpyridine-Zn^{2+} moiety. Therefore, the red-shifted fluorescence and absorption were observed because the energy level of the lowest unoccupied molecular orbital decreased more than that of the highest occupied molecular orbital upon complexation with Zn^{2+} (Shiraishi et al., 2011).

Figure 2-(a) shows the fluorescence spectral change in the fluoroionophore with increasing concentrations of Zn^{2+}. The original strong fluorescence band at 539 nm (F_{539}) gradually decreased, and a new fluorescence peak at 567 nm (F_{567}) appeared and increased. The spectral change was largely terminated by the addition of 200 eq. of Zn^{2+}. This red-shift of the spectra enabled ratiometric measurement by calculating the ratio of F_{567} to F_{539}. Ratiometric fluoroionophores are more favorable for quantitative determination than those exhibiting only fluorescence enhancement (“turn-on”) or fluorescence quenching (“turn-off”) because the ratio of the fluorescence intensities is independent of fluctuation of the source light intensity and sensitivity of the instrument (Valeur, 2002). The ratio of fluorescence intensities at 567 nm and 539 nm (F_{567}/F_{539}) increased as the Zn^{2+} concentration increased (Figure 2-(b)), and the sigmoidal plot generated enabled quantitative determination of Zn^{2+}. Job’s method was used to further investigate the binding stoichiometry of the fluoroionophore and Zn^{2+} (Connars, 1987). In

solutions in which the total concentration of the fluoroionophore and Zn^{2+} was maintained at 4 μM, F_{567} was highest when the mole fraction of Zn^{2+} was 0.5, suggesting 1:1 stoichiometry (Figure 2-(c)). Furthermore, we calculated a dissociation constant (K_d) of 4.36×10^{-6} M for Zn^{2+} using a Benesi-Hildebrand plot (Figure 2-(d)) (Benesi et al., 1949).

3.2 Effect of metal ions, pH and DOC on the fluoroionophore

To assess the selectivity of the fluoroionophore toward Zn^{2+}, the interfering effects of various ions were investigated. In this selectivity test, the concentrations of each ion solution were set higher than those in real urban runoff samples described below. As shown in Figure 3, Na^{+}, Mg^{2+}, K^{+}, and Ca^{2+} did not influence the fluorescence intensity ratio (F_{567}/F_{539}) of the fluoroionophore. In addition, no change in F_{567}/F_{539} was observed upon addition of Al^{3+}, Mn^{2+}, Fe^{3+}, and Pb^{2+}. In contrast, F_{567}/F_{539} increased significantly in Hg^{2+} and Cd^{2+} solutions. It is difficult for most ionophores to discriminate Cd^{2+}, Hg^{2+}, and Zn^{2+} because they have similar chemical properties (Li et al., 2012). However, further addition of Zn^{2+} to the solutions resulted in further increases in the ratio (F_{567}/F_{539}), and these spectra overlapped those of Zn^{2+}, indicating that the fluoroionophore has much greater selectivity for Zn^{2+} than Cd^{2+} and Hg^{2+}. These characteristics of the fluoroionophore are advantageous for analysis of Zn^{2+} in environmental aquatic samples. Addition of Fe^{2+}, Co^{2+}, Ni^{2+}, and Cu^{2+} quenched the fluorescence. Interestingly, the fluorescent signals of Co^{2+} and Ni^{2+} solutions were recovered by the addition of Zn^{2+}, suggesting that Co^{2+} and Ni^{2+} do not significantly affect recognition of Zn^{2+} by the fluoroionophore. Fe and Cu are known to efficiently

quench fluorescence. Specifically, when these heavy metal ions are bound to fluoroionophores, fluorescence quenching is usually observed owing to an energy or electron transfer mechanism (e.g., paramagnetic Cu^{2+}) (Varnes et al., 1972).

The pH of a sample solution usually affects fluorescence spectra because of the protonation reaction of a fluoroionophore (Valeur, 2002). Therefore, the pH dependence of the fluoroionophore was investigated at pH 1.5–9.0 (Figure 4). In solutions with a pH < 3.5, the F_{567}/F_{539} of the fluoroionophore increased with decreasing pH owing to decreasing fluorescence intensity at 539 nm. These findings might be attributed to di-protonation of the terpyridine unit (Resch-Genger et al., 2006). In solutions with a pH of 4.0–9.0, the pH value did not affect the fluorescence of the fluoroionophore, and F_{567}/F_{539} was stable. Hence, there was no need to control the pH of the sample solutions unless it was below pH 4.0.

To investigate the interference effect of organic matter on the fluorescence determination of Zn^{2+}, fluorescence titration with NOM was conducted (Figure 5). NOM did not affect the F_{567}/F_{539} of the samples without Zn^{2+}, which suggested NOM does not interfere with the fluorescence of the fluoroionophore. In the presence of Zn^{2+}, the F_{567}/F_{539} gradually decreased with increasing DOC concentration. The F_{567}/F_{539} decreased 16% at 5.9 mg-DOC/L. This result revealed organic matter can affect the fluorescence determination of Zn^{2+} because it can bind to Zn^{2+}.

3.3 Determination of Zn^{2+} concentrations in urban runoff samples

Prior to measurement of the fluorescence of urban runoff samples with different concentrations of Zn^{2+}, the concentrations of a variety of metals, pH, and EC in the

254 samples were determined (Table 1). The T-Zn concentrations in most of the samples were
255 above the environmental quality standard. Samples collected in Osaka contained higher
256 concentrations of Zn than those from other cities, which was likely due to the heavy
257 traffic load of Osaka. Most of the samples contained high concentrations of Al and Fe (up
258 to 2600 μg/L and 3500 μg/L, respectively); however, Cd was not detected in all samples.
259 The pH values of the samples were around 7.0 for all cities. The EC values were high for
260 samples from Osaka and low for those taken in Tsukuba. Table 2 shows the
261 concentrations of the dissolved fraction of metals, pH, and DOC. The Al concentrations
262 were relatively high in the samples collected in Osaka, Gifu, and East-Hiroshima.
263 Especially, one sample of Osaka city contained 720 μg-Al/L. The Zn concentrations of
264 were higher up to 140 μg/L in the samples taken at Osaka than those taken at other cities.
265 The Cu concentrations were over 100 μg/L in the three samples. Almost all the samples
266 included Fe at tens of μg/L level. Among the four sampling sites, dissolved metal
267 concentrations were lowest in Tsukuba. Pb and Cd were not detected in all samples.
268 When compared with the T-Zn concentrations (Table 1), D-Zn accounted for 32% of the
269 T-Zn on average. Taken together, these findings indicate a great diversity of chemical
270 compositions among samples.
271 Following ICP analysis, we measured Zn concentrations in the same urban runoff
272 samples using the fluoroionophores. To accomplish this, we generated a calibration curve
273 of Zn^{2+} from analysis of Zn standard solutions prepared with Milli-Q water by plotting
274 fluorescence intensity ratios (F_{567}/F_{539}) of the fluoroionophore in standard solutions
275 containing 0–2.5 μM of Zn^{2+} (Figure 5). The calibration curve was fitted by a quartic
276 function ($F_{567}/F_{539} = 1.51 \times [Zn^{2+}]^4 + 0.87 \times [Zn^{2+}]^2 + 0.28$) because it produced a better

277 determination coefficient (R^2 = 0.9996) than quadratic and cubic functions. The detection
278 limit was 1.4×10^{-7} M (9 μg/L), which was sufficiently low for screening of Zn in many
279 environmental and industrial aqueous samples.

280 The applicability of fluorescence spectroscopy to measurement of Zn in urban
281 runoff samples was investigated. As shown in Tables 1 and 2, 25 real urban runoff
282 samples were collected from four cities in Japan and the Zn concentrations were
283 determined by the proposed fluorescence spectroscopy (C_{flu}) method and conventional
284 ICP-AES (C_{ICP}) to determine whether the developed method is applicable to analysis of
285 actual urban runoff samples. Figure 6 shows relationship between concentrations of
286 D-Zn and T-Zn in urban runoff samples determined by fluorescence spectroscopy and
287 ICP measurements. The results revealed an almost linear relationship with a slope of 1,
288 indicating that the fluoroionophore is applicable to determination of Zn in environmental
289 samples with complex matrices. The relative errors in the concentrations of D-Zn
290 determined by these two methods were within 25% for most samples. Errors in the
291 concentrations of T-Zn were within 30% for most samples; thus, we concluded that T-Zn
292 as well as D-Zn in urban runoff samples was successfully determined by using our new
293 fluorescence method with simple pretreatments.

294 However, there were some limitations of the fluorescence method; (1) T-Zn was
295 not detected by fluorescence spectroscopy in two samples collected from East-Hiroshima,
296 even though those were detected by ICP-AES analysis. (2) The fluorescence method
297 overestimated D-Zn in samples collected in Tsukuba. (3) On the whole, the fluorescence
298 spectroscopy tended to underestimate T-Zn concentrations. It is likely that, because Zn
299 complexes that remained in the samples were more stable than complexes of the

300 terpyridine receptor in the fluoroionophore with Zn^{2+} (Scheinost et al., 2002), the
301 fluoroionophore could not remove Zn from the complexes. It is known that Zn^{2+} can bind
302 to organic matter (Figure 5) or that Zn exists as an inorganic compound in aqueous
303 environmental systems (Priadi et al., 2012). The results presented here suggest that the
304 Zn species in an aqueous sample can be fractionated using a set of BODIPY derivatives
305 with metal ion ligands that have different binding constants.
306 We conducted Spearman's rank correlation analysis to investigate interfering
307 effects of organic and inorganic matter in the samples (Tables 1 and 2). A two-tailed test
308 at the 1% significance level revealed no significant components selected in this study
309 (Tables 1 and 2) that interfered with fluorescence measurements of D-Zn. Conversely,
310 the Spearman rank-correlation coefficients (r_s) of Mn, Ni, and Pb toward T-Zn
311 quantification were 0.525, 0.728, and 0.519, respectively (Table 3), which were
312 significant (> 0.01), indicating that these three metals had the potential to affect the
313 fluorescence measurements of T-Zn in urban runoff samples. However, the selectivity
314 test revealed that these metals did not inhibit the fluorescence of the fluoroionophore
315 (Figure 3). Our data analysis also indicated that the interfering effects of the sample
316 matrix, especially organic matter, Cu and Fe present in the samples (Tables 1 and 2), were
317 negligible, even though the fluoroionophore was quenched by the addition of Cu and Fe
318 (Figure 3), and Zn^{2+} could bind to organic matter (Figure 5). These findings indicate that
319 other interfering components for fluorescence measurements of Zn could exist in the
320 samples.
321
322 **4. Conclusions**

In this study, we demonstrated the potential for application of fluorescence spectroscopy for measurement of T-Zn and D-Zn in real environmental samples using a fluoroionophore based on a BODIPY-terpyridine conjugate. The presented approach is easy to use and requires no special pretreatment. We also showed potential effects of other metal ions, pH, and DOC as interfering substances. Further research about Zn species in aqueous environment and interfering effects of sample matrix are needed to solve the limitations of the new method. Fluorescence detection has great promise for onsite, rapid screening of toxic metals, as well as monitoring of other anthropogenic pollutants in aquatic environments.

Acknowledgements

This research was financially supported by Grants-in-Aid for Scientific Research (No. 12J01817 and No. 23686074) from the Japan Society for the Promotion of Science. This study was also partially supported by the Core Research of Evolutional Science and Technology (CREST) for Innovative Technology and Systems for Sustainable Water Use from the Japan Science and Technology Agency (JST). We thank Dr. Hideaki Maki, Dr. Shinsuke Kasahara, Dr. Toshiro Yamada, and Dr. Tomonori Kindaichi for providing us with urban runoff samples and Dr. Nobutaka Shirasaki for advice on the experimental design.

References

Adeloju, S. B., Zhang, Y., 2009. Vapor Generation Atomic Absorption Spectrometric Determination of Cadmium in Environmental Samples with In-Line Anion Exchange

346 Separation. Analytical Chemistry 81(11), 4249-4255.
347 Benesi, H. A., Hildebrand, J. H., 1949. A SPECTROPHOTOMETRIC
348 INVESTIGATION OF THE INTERACTION OF IODINE WITH AROMATIC
349 HYDROCARBONS. Journal of the American Chemical Society 71(8), 2703-2707.
350 Bischel, H. N., Simon, G. L., Frisby, T. M., Luthy, R. G., 2012. Management Experiences
351 and Trends for Water Reuse Implementation in Northern California. Environmental
352 Science & Technology 46(1), 180-188.
353 Connars, K. A., 1987. Binding Constants. Wiley-Interscience, New York.
354 Domaille, D. W., Que, E. L., Chang, C. J., 2008. Synthetic fluorescent sensors for
355 studying the cell biology of metals. Nature Chemical Biology 4(3), 168-175.
356 Gong, J., Zhou, T., Song, D., Zhang, L., Hu, X., 2010. Stripping Voltammetric Detection
357 of Mercury(II) Based on a Bimetallic Au-Pt Inorganic-Organic Hybrid
358 Nanocomposite Modified Glassy Carbon Electrode. Analytical Chemistry 82(2),
359 567-573.
360 Hafuka, A., Taniyama, H., Son, S. H., Yamada, K., Takahashi, M., Okabe, S., Satoh, H.,
361 2013. BODIPY-based ratiometric fluoroionophores with bidirectional spectral shifts
362 for the selective recognition of heavy metal ions. Bulletin of the Chemical Society of
363 Japan 86(1), 37-44.
364 Han, Z. X., Zhang, X. B., Zhuo, L., Gong, Y. J., Wu, X. Y., Zhen, J., He, C. M., Jian, L. X.,
365 Jing, Z., Shen, G. L., Yu, R. Q., 2010. Efficient Fluorescence Resonance Energy
366 Transfer-Based Ratiometric Fluorescent Cellular Imaging Probe for Zn^{2+} Using a
367 Rhodamine Spirolactam as a Trigger. Analytical Chemistry 82(8), 3108-3113.
368 Henderson, R. K., Baker, A., Murphy, K. R., Hamblya, A., Stuetz, R. M., Khan, S. J.,

2009. Fluorescence as a potential monitoring tool for recycled water systems: A review. Water Research 43(4), 863-881.

Hong, Y., Chen, S., Leung, C. W. T., Lam, J. W. Y., Liu, J., Tseng, N. W., Kwok, R. T. K., Yu, Y., Wang, Z., Tang, B. Z., 2011. Fluorogenic Zn(II) and Chromogenic Fe(II) Sensors Based on Terpyridine-Substituted Tetraphenylethenes with Aggregation-Induced Emission Characteristics. Acs Applied Materials & Interfaces 3(9), 3411-3418.

Japanese Ministry of Environment, Environmental quality standards for water pollution. http://www.env.go.jp/en/water/wq/wp.pdf

Karolin, J., Johansson, L. B. A., Strandberg, L., Ny, T., 1994. FLUORESCENCE AND ABSORPTION SPECTROSCOPIC PROPERTIES OF DIPYRROMETHENEBORON DIFLUORIDE (BODIPY) DERIVATIVES IN LIQUIDS, LIPID-MEMBRANES, AND PROTEINS. Journal of the American Chemical Society 116(17), 7801-7806.

Lakowicz, J. R., 2006. Principles of Fluorescence Spectroscopy. 3rd ed, Springer, New York.

Li, C. Y., Zhang, X. B., Qiao, L., Zhao, Y., He, C. M., Huan, S. Y., Lu, L. M., Jian, L. X., Shen, G. L., Yu, R. Q., 2009. Naphthalimide-Porphyrin Hybrid Based Ratiometric Bioimaging Probe for Hg^{2+}: Well-Resolved Emission Spectra and Unique Specificity. Analytical Chemistry 81(24), 9993-10001.

Li, M., Lu, H. Y., Liu, R. L., Chen, J. D., Chen, C. F., 2012. Turn-On Fluorescent Sensor for Selective Detection of Zn^{2+}, Cd^{2+}, and Hg^{2+} in Water. Journal of Organic Chemistry 77(7), 3670-3673.

Li, Z., Xiang, Y., Tong, A., 2008. Ratiometric chemosensor for fluorescent determination of Zn^{2+} in aqueous ethanol. Analytica Chimica Acta 619(1), 75-80.

Liang, L. J., Zhao, X. J., Huang, C. Z., 2012. Zn(II) complex of terpyridine for the highly selective fluorescent recognition of pyrophosphate. Analyst 137(4), 953-958.

Loudet, A., Burgess, K., 2007. BODIPY dyes and their derivatives: Syntheses and spectroscopic properties. Chemical Reviews 107(11), 4891-4932.

Mahbub, P., Ayoko, G. A., Goonetilleke, A., Egodawatta, P., Kokot, S., 2010. Impacts of Traffic and Rainfall Characteristics on Heavy Metals Build-up and Wash-off from Urban Roads. Environmental Science & Technology 44(23), 8904-8910.

Majedi, S. M., Lee, H. K., Kelly, B. C., 2012. Chemometric Analytical Approach for the Cloud Point Extraction and Inductively Coupled Plasma Mass Spectrometric Determination of Zinc Oxide Nanoparticles in Water Samples. Analytical Chemistry 84(15), 6546-6552.

Naito, W., Kamo, M., Tsushima, K., Iwasaki, Y., 2010. Exposure and risk assessment of zinc in Japanese surface waters. Science of the Total Environment 408(20), 4271-4284.

Olmsted, J., 1979. CALORIMETRIC DETERMINATIONS OF ABSOLUTE FLUORESCENCE QUANTUM YIELDS. Journal of Physical Chemistry 83(20), 2581-2584.

Piao, X., Zou, Y., Wu, J., Li, C., Yi, T., 2009. Multiresponsive Switchable Diarylethene and Its Application in Bioimaging. Organic Letters 11(17), 3818-3821.

Priadi, C., Le Pape, P., Morin, G., Ayrault, S., Maillot, F., Juillot, F., Hochreutener, R., Llorens, I., Testemale, D., Proux, O., Brown, G. E., 2012. X-ray Absorption Fine

Structure Evidence for Amorphous Zinc Sulfide as a Major Zinc Species in Suspended Matter from the Seine River Downstream of Paris, Ile-de-France, France. Environmental Science & Technology 46(7), 3712-3720.

Resch-Genger, U., Li, Y. Q., Bricks, J. L., Kharlanov, V., Rettig, W., 2006. Bifunctional charge transfer operated fluorescent probes with acceptor and donor receptors. 1. Biphenyl-type sensor molecules with protonation-induced anti-energy gap rule behavior. Journal of Physical Chemistry A 110(38), 10956-10971.

Rosner, B., 2011. Fundamentals of Biostatistics. 7th edition, Duxbury Press, Pacific Grove.

Scheinost, A. C., Kretzschmar, R., Pfister, S., Roberts, D. R., 2002. Combining selective sequential extractions, x-ray absorption spectroscopy, and principal component analysis for quantitative zinc speciation in soil. Environmental Science & Technology 36(23), 5021-5028.

Shiraishi, Y., Ichimura, C., Sumiya, S., Hirai, T., 2011. Multicolor Fluorescence of a Styrylquinoline Dye Tuned by Metal Cations. Chemistry-a European Journal 17(30), 8324-8332.

Valeur, B., 2002. Molecular Fluorescence: Principles and Applications. Wiley-VCH, Weinheim.

Varnes, A. W., Wehry, E. L., Dodson, R. B., 1972. INTERACTIONS OF TRANSITION-METAL IONS WITH PHOTOEXCITED STATES OF FLAVINS - FLUORESCENCE QUENCHING STUDIES. Journal of the American Chemical Society 94(3), 946-950.

Weng, Y., Chen, Z., Wang, F., Xue, L., Jiang, H., 2009. High sensitive determination of

zinc with novel water-soluble small molecular fluorescent sensor. Analytica Chimica Acta 647(2), 215-218.

Yan, J., Indra, E. M., 2012. Colorimetric Method for Determining Pb^{2+} Ions in Water Enhanced with Non-Precious-Metal Nanoparticles. Analytical Chemistry 84(14), 6122-6127.

Figure and table captions

Figure 1. (A) Absorption (gray) and fluorescence (black) spectra of the fluoroionophore (1 μM) with (solid line) and without (dashed line) Zn^{2+} (100 μM). The excitation wavelength was 535 nm. (B) Absorption (left) and fluorescence (right) of the fluoroionophore with and without Zn^{2+}, respectively.

Figure 2. (A) Change in the fluorescence spectra of the fluoroionophore (1 μM) with increasing Zn^{2+} concentrations. The spectra shown are for Zn^{2+} concentrations of 0, 0.2, 0.4, 0.6, 0.8, 1.0, 1.2, 1.4, 1.6, 2.0, 2.4, 3.0, 4.0, 6.0, 10.0, 14.0, 16.0, 20.0, 40.0, 100.0, and 200.0 μM. The excitation wavelength was 535 nm. (B) Plot of the fluorescence intensity ratio (F_{567}/F_{539}) versus increasing concentrations of Zn^{2+}. The concentration of the fluoroionophore was 1 μM and the excitation wavelength was 535 nm. (C) Job's plot of the fluoroionophore and Zn^{2+} system. The total concentration was 4 μM and the fluorescence intensity was measured at 567 nm. (D) Benesi-Hildebrand plot of fluorescence intensity at 539 nm.

Figure 3. Changes in the fluorescence intensity ratio (F_{567}/F_{539}) upon addition of different metal ions. White bars represent the addition of an excess of a metal ion (10 μM) to a 1 μM solution of the fluoroionophore. Black bars represent the subsequent addition of 10 μM of Zn^{2+} to a solution with each metal ion. Excitation was provided at 535 nm.

Figure 4. Effect of pH on the fluorescence intensity ratio (F_{567}/F_{539}) of the

fluoroionophore.

Figure 5. Effect of DOC on the fluorescence intensity ratio (F_{567}/F_{539}) of the fluoroionophore with (circles) and without (squares) Zn^{2+}. Zn^{2+} concentration was kept constant at 10 μM.

Figure 6. Curve of fluorescence intensity ratio (F_{567}/F_{539}) of the fluoroionophore at Zn^{2+} concentrations below 2.5 μM.

Figure 7. Relationship between concentrations of D-Zn (A) and T-Zn (B) in urban runoff samples determined by fluorescence spectroscopy with the fluoroionophore and by ICP measurements. Samples were taken in Osaka (circles), Tsukuba (crosses), Gifu (triangles), and East-Hiroshima (squares).

Table 1. Concentrations of metals (μg/L), pH, and EC (mS/cm) in urban runoff samples.

Table 2. Concentrations of dissolved fraction of metals (μg/L), pH, and DOC (mg/L) in urban runoff samples.

Table 3. r_s, t, and P values of metals, protons, and EC toward T-Zn concentration errors.

Graphical Abstract

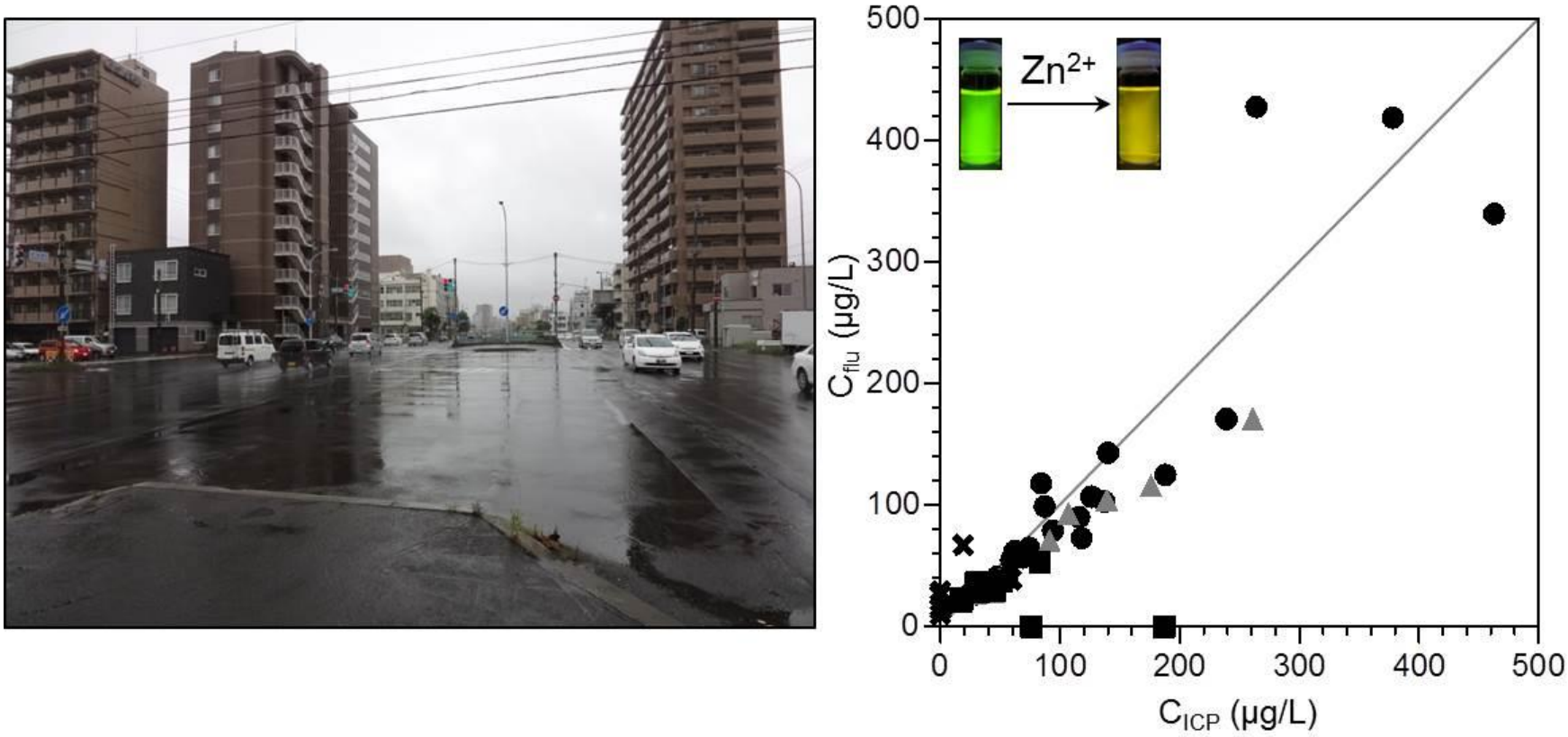

Figure 1.

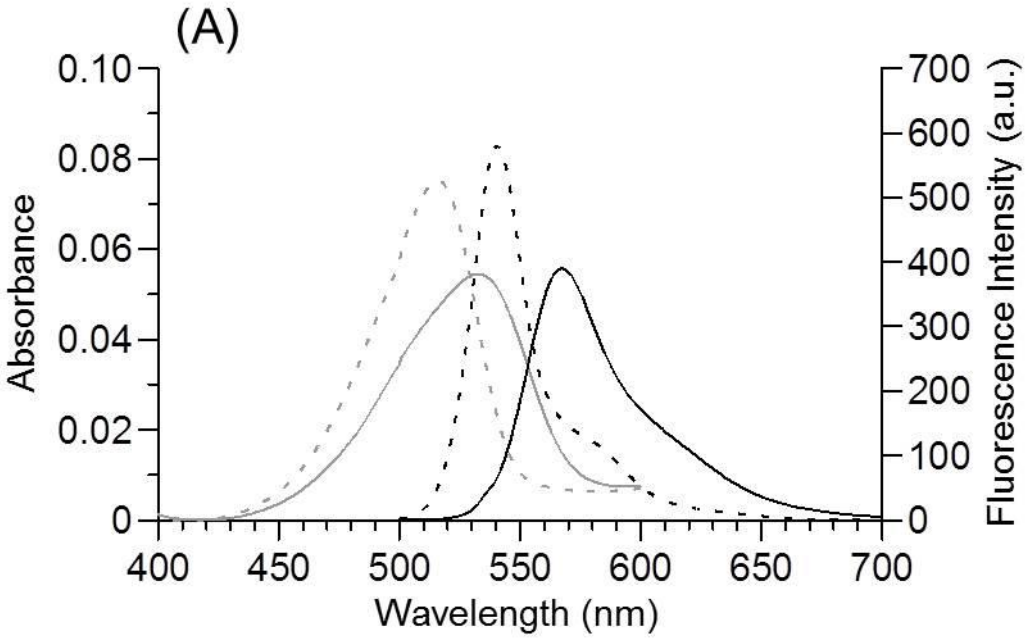
(A)
Absorbance
Fluorescence Intensity (a.u.)
Wavelength (nm)
0.10
0.08
0.06
0.04
0.02
0
700
600
500
400
300
200
100
0
400
450
500
550
600
650
700

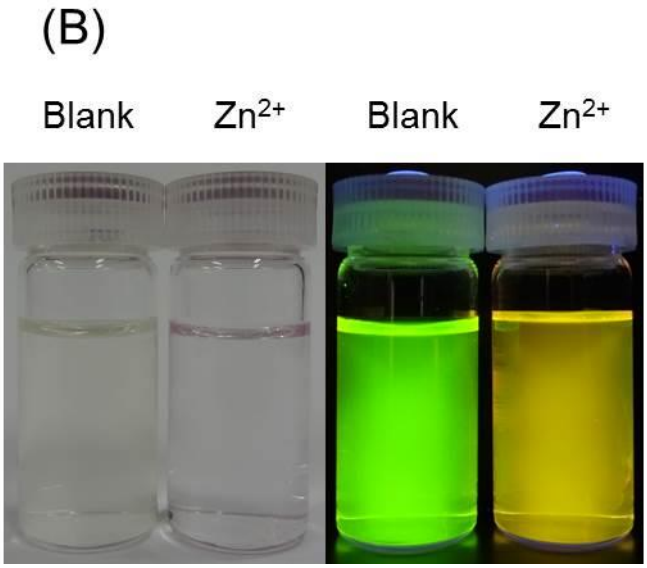
(B)
Blank
Zn2+
Blank
Zn2+

Figure 2.

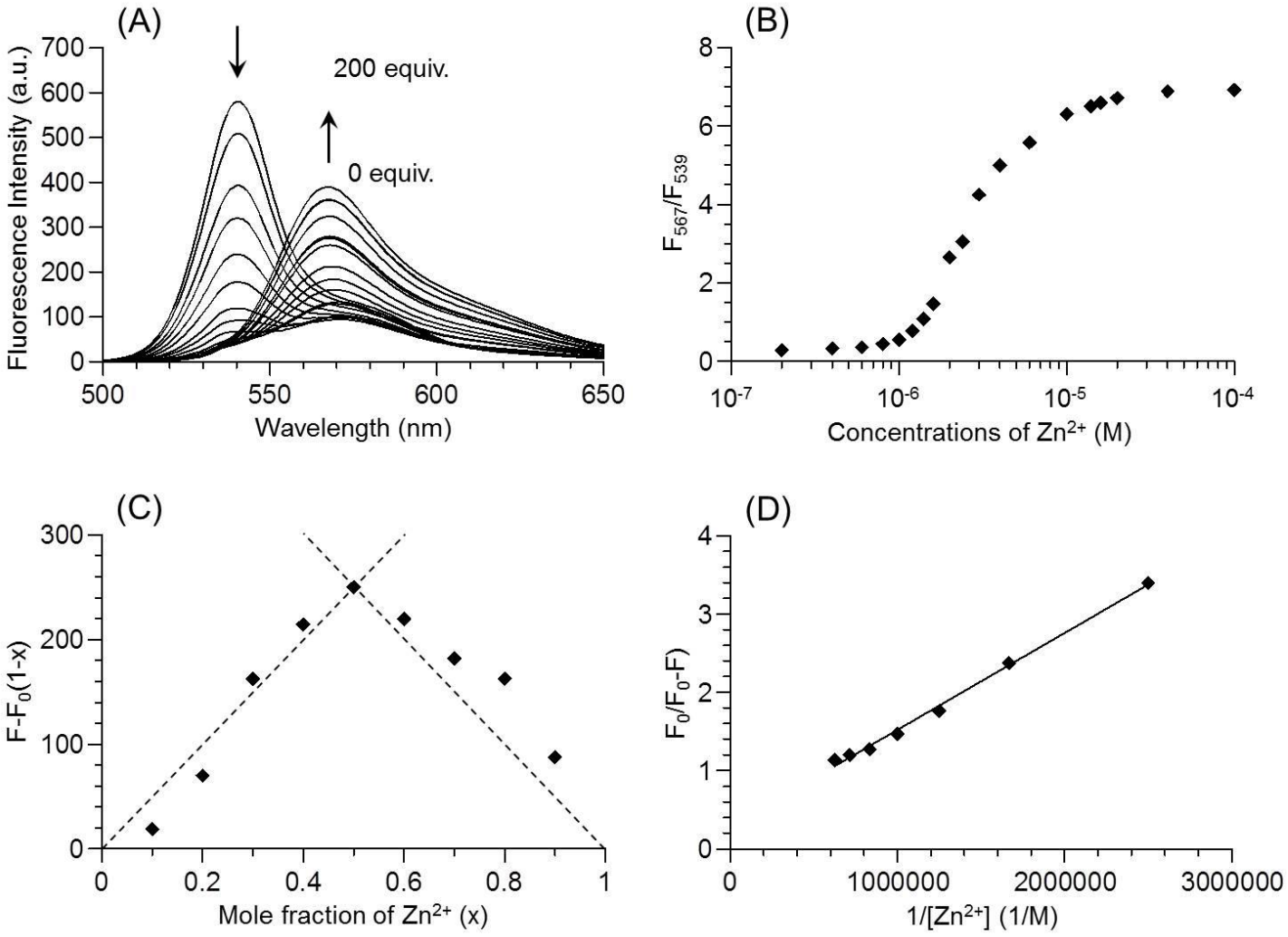
(A)
200 equiv.
0 equiv.
Fluorescence Intensity (a.u.)
Wavelength (nm)
(B)
F_{567}/F_{539}
Concentrations of Zn^{2+} (M)
(C)
$F-F_0(1-x)$
Mole fraction of Zn^{2+} (x)
(D)
$F_0/F_0-F)$
$1/[Zn^{2+}]$ (1/M)

Figure 3.

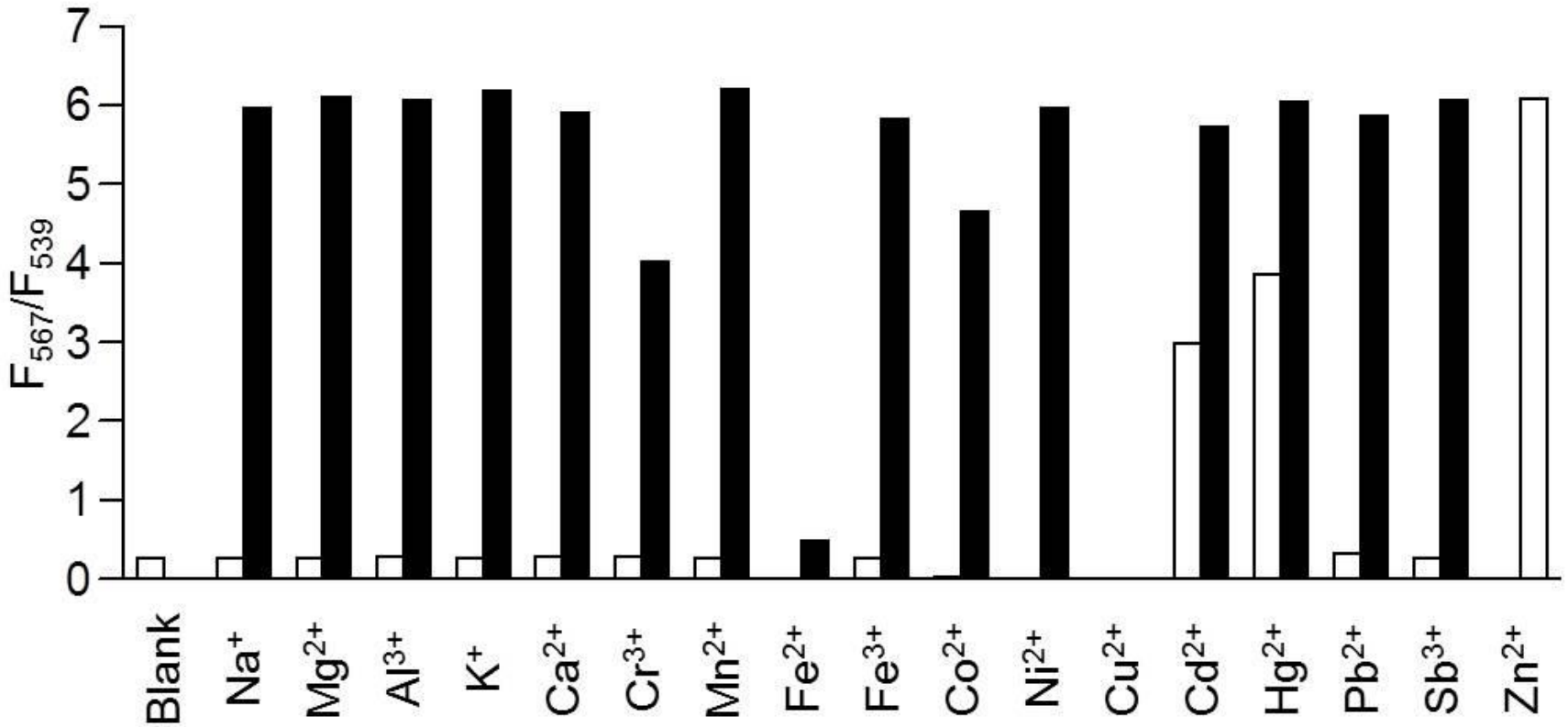
F_{567}/F_{539}
0
1
2
3
4
5
6
7
Blank
Na^{+}
Mg^{2+}
Al^{3+}
K^{+}
Ca^{2+}
Cr^{3+}
Mn^{2+}
Fe^{2+}
Fe^{3+}
Co^{2+}
Ni^{2+}
Cu^{2+}
Cd^{2+}
Hg^{2+}
Pb^{2+}
Sb^{3+}
Zn^{2+}

Figure 4.

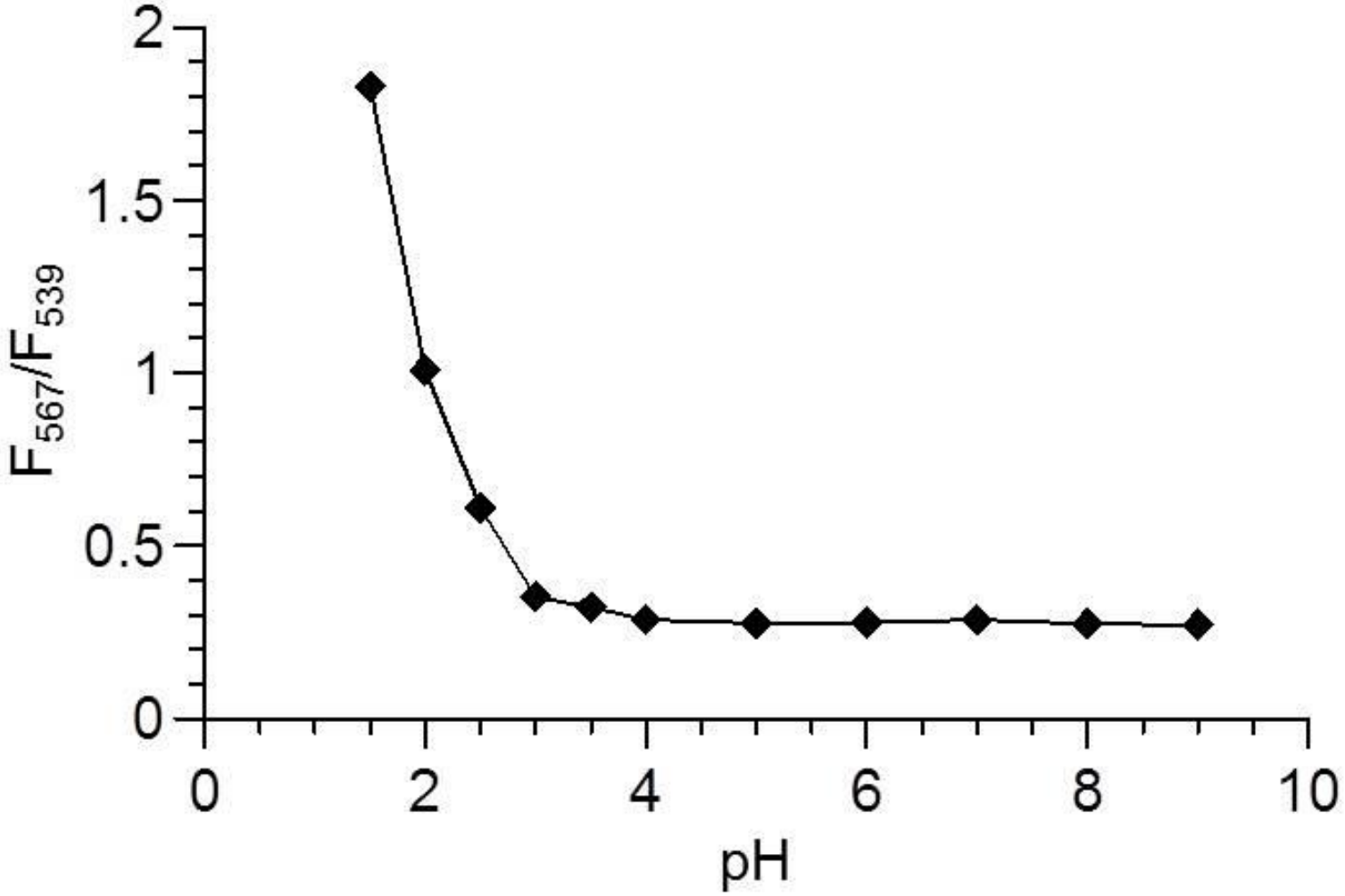

Figure 5.

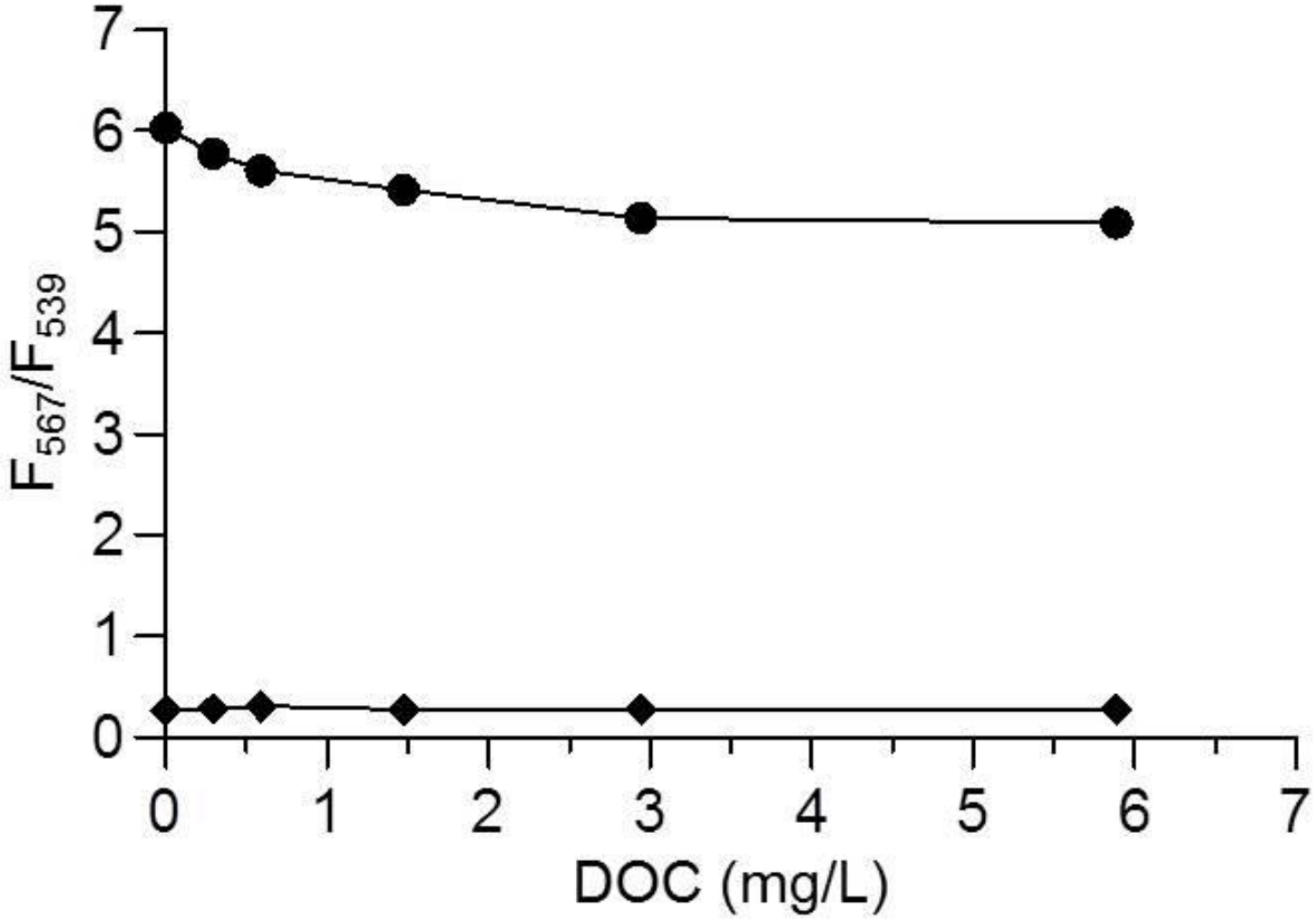

Figure 6.

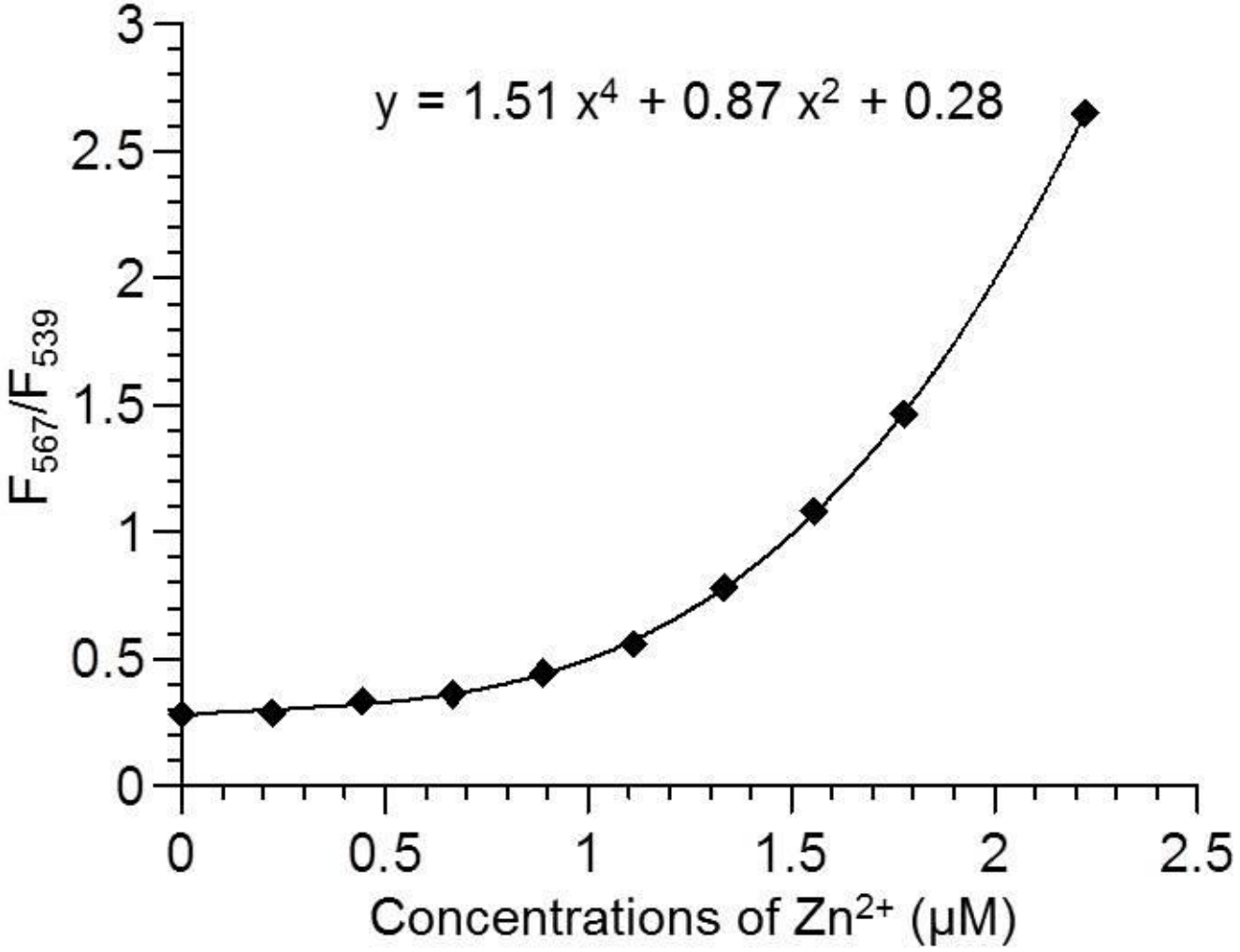
y = 1.51 x4 + 0.87 x2 + 0.28
F567/F539
Concentrations of Zn2+ (μM)
0
0.5
1
1.5
2
2.5
3

Figure 7..

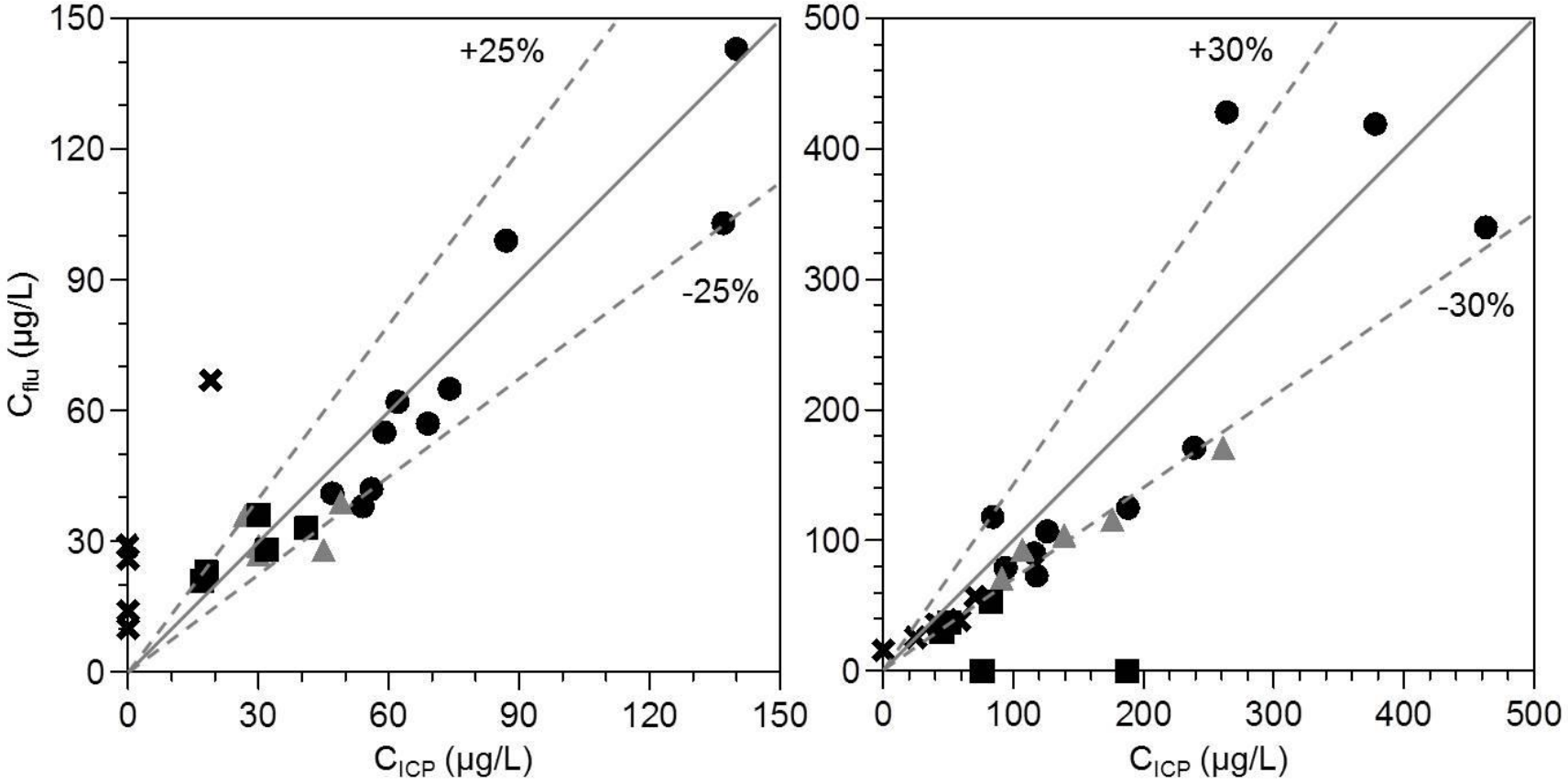
150
120
90
60
30
0
0
30
60
90
120
150
+25%
-25%
C_{flu} (µg/L)
C_{ICP} (µg/L)
500
400
300
200
100
0
0
100
200
300
400
500
+30%
-30%
C_{ICP} (µg/L)

Table 1. Concentrations of metals (μg/L), pH, and EC (mS/cm) in urban runoff samples.

City	Sample No.	Zn	Al	Cd	Cr	Cu	Fe	Mn	Ni	Pb	Sb	pH	EC
Osaka	1	264	800	ND	4	122	488	56	13	ND	6	6.92	18.8
	2	126	142	ND	2	60	131	5	5	ND	6	6.80	10.7
	3	116	408	ND	4	ND	413	16	3	14	ND	7.03	19.4
	4	118	317	ND	2	ND	484	26	2	10	ND	6.94	2.0
	5	188	596	ND	5	ND	1026	32	5	11	ND	7.42	1.9
	6	94	119	ND	1	ND	287	15	3	ND	ND	6.76	9.2
	7	239	517	ND	5	36	1016	41	6	ND	6	6.90	10.9
	8	84	233	ND	1	ND	422	15	3	ND	ND	7.42	9.0
	9	378	1071	ND	7	104	2322	64	11	22	7	6.80	9.6
	10	463	1689	ND	9	68	3544	95	11	26	8	6.98	7.7
Tsukuba	1	59	1411	ND	5	ND	1144	31	ND	12	8	6.87	5.0
	2	25	1200	ND	4	ND	1244	34	ND	ND	9	6.90	6.1
	3	ND	367	ND	3	ND	512	18	ND	ND	ND	7.12	5.9
	4	41	1256	ND	4	ND	1433	47	ND	ND	ND	6.72	5.8
	5	71	1093	ND	6	ND	1400	39	ND	ND	7	7.10	6.3
Gifu	1	261	1678	ND	5	420	1944	83	4	12	7	7.20	8.8
	2	176	670	ND	2	158	871	33	2	ND	ND	6.98	8.5
	3	107	728	ND	2	119	784	32	ND	ND	ND	6.98	9.0
	4	91	706	ND	2	711	489	18	ND	10	ND	7.12	8.7
	5	139	971	ND	2	337	946	36	ND	ND	ND	6.56	8.4
East-Hiroshima	1	76	1433	ND	6	78	1478	53	2	16	ND	6.50	10.9
	2	187	2600	ND	10	266	2911	96	4	34	5	7.03	10.8
	3	51	480	ND	2	411	552	20	ND	ND	ND	6.97	9.8
	4	45	534	ND	3	289	574	21	ND	11	4	6.45	11.1
	5	83	580	ND	3	154	574	23	2	ND	5	6.67	10.9

ND: Not detected.

Table 2. Concentrations of dissolved fraction of metals (μg/L), pH, and DOC (mg/L) in urban runoff samples.

City	Sample No.	Zn	Al	Cd	Cr	Cu	Fe	Mn	Ni	Pb	Sb	pH	DOC
Osaka	1	140	158	ND	2	112	54	45	12	ND	7	6.92	59.8
	2	74	ND	ND	1	32	16	4	5	ND	5	6.80	24.3
	3	47	292	ND	2	ND	15	7	2	ND	ND	7.03	2.4
	4	54	720	ND	ND	ND	24	7	2	ND	ND	6.94	1.5
	5	56	126	ND	ND	ND	13	6	2	ND	ND	7.42	1.6
	6	62	ND	ND	ND	ND	22	8	2	ND	ND	6.76	2.7
	7	137	654	ND	2	ND	63	19	4	ND	ND	6.90	10.5
	8	59	81	ND	ND	ND	18	8	3	ND	ND	7.42	9.8
	9	69	ND	ND	ND	70	18	16	7	ND	ND	6.80	32.4
	10	87	ND	ND	ND	ND	14	23	5	ND	6	6.98	15.4
Tsukuba	1	19	ND	ND	4	ND	15	6	ND	ND	5	6.87	0.8
	2	ND	ND	ND	2	ND	13	8	ND	ND	6	6.90	1.5
	3	ND	ND	ND	ND	ND	ND	ND	ND	ND	ND	7.12	1.4
	4	ND	ND	ND	2	ND	5	5	ND	ND	5	6.72	1.1
	5	ND	ND	ND	4	ND	9	7	ND	ND	18	7.10	1.2
Gifu	1	45	201	ND	ND	152	99	17	ND	ND	4	7.20	3.3
	2	49	169	ND	ND	73	78	8	ND	ND	6	6.98	2.4
	3	30	284	ND	ND	ND	20	5	ND	ND	ND	6.98	0.9
	4	27	102	ND	ND	ND	36	4	ND	ND	ND	7.12	1.9
	5	30	91	ND	ND	ND	54	3	ND	ND	ND	6.56	0.9
East-Hiroshima	1	41	289	ND	1	20	23	7	ND	ND	ND	6.50	2.7
	2	32	249	ND	1	136	71	8	ND	ND	ND	7.03	7.2
	3	17	85	ND	1	63	17	4	ND	ND	ND	6.97	1.8
	4	18	81	ND	1	22	16	5	ND	ND	ND	6.45	1.7
	5	30	109	ND	1	92	35	7	ND	ND	ND	6.67	11.6

ND: Not detected

Table 3. r_s, t, and P values of metals, protons, and EC toward T-Zn concentration errors.

	Al	Cd	Cr	Cu	Fe	Mn	Ni	Pb	Sb	H^+	EC
r_s	0.292	0.000	0.412	0.300	0.281	0.525	0.728	0.519	0.118	-0.180	0.233
t	1.466	0.000	2.168	1.511	1.403	2.961	5.091	2.909	0.568	-0.877	1.150
P	0.156	1.000	0.041	0.144	0.174	0.007	0.000	0.008	0.575	0.389	0.262

For submission to Water Research as a **Research Paper**

Supporting Information

Application of Fluorescence Spectroscopy Using a Novel Fluoroionophore for Quantification of Zinc in Urban Runoff

Akira Hafuka[a], Hiroaki Yoshikawa[a], Koji Yamada[b], Tsuyoshi Kato[c], Masahiro Takahashi[a], Satoshi Okabe[a], and Hisashi Satoh[a,*]

[a] Division of Environmental Engineering, Graduate School of Engineering, Hokkaido University, North-13, West-8, Sapporo 060-8628, Japan

[b] Division of Environmental Materials Science, Graduate School of Environmental Science, Hokkaido University, North-10, West-5, Sapporo 060-0810, Japan

[c] Department of Computer Science, Graduate School of Engineering, Gunma University, 1-5-1 Tenjin-cho, Kiryu 376-8515, Japan

Procedure of data analysis for obtaining Spearman rank correlation coefficients

To investigate the interference effects on fluorescence measurements of Zn in urban runoff samples, Spearman rank correlation coefficients for metals, protons, DOC, and EC were computed. The procedure for computing the Spearman rank correlation coefficient is described as follows.

Assume we have n observations, $X_1, X_2, \ldots, X_n$, each of which is the absolute difference between a Zn concentration determined by ICP and that of fluoroionophore. In this study, the number of observations was $n = 25$. Another data set, $Y_1, Y_2, \ldots, Y_n$, is also given, where Y_i is paired with X_i. The data, $Y_1, Y_2, \ldots, Y_n$, were of one of ten metals including Zn, Al, Cd, Cr, Cu, Fe, Mn, Ni, Pb, and Sb.

These n data, X_is and Y_is, are converted to ranks, x_is and y_is, respectively. The Spearman rank correlation coefficient was then defined as:

$$r_s = \frac{\sum_{i=1}^{n}(x_i - \bar{x})(y_i - \bar{y})}{\sqrt{\sum_{i=1}^{n}(x_i - \bar{x})^2}\sqrt{\sum_{i=1}^{n}(y_i - \bar{y})^2}}$$

where $\bar{x}$ and $\bar{y}$ are the average of x_is and y_is. Because x_is and y_is are ranks, the equalities of $\bar{x} = \bar{y} = (n + 1)/2$ are always established.

Spearman rank correlation coefficients are in the range of −1 to +1, with correlation coefficients further from zero implying strong relationships between X_is and Y_is and those closer to zero indicating weak relationships. However, the absolute correlation coefficients become large when there are few observations, suggesting that the relationships between two variables cannot be discussed based on only the Spearman rank correlation coefficient. Therefore, statistical hypothesis tests were performed to address this issue. If X_is are statistically independent of Y_is, the subsequent value follows the Student's t-test distribution with $(n - 2)$ degrees of freedom under some natural assumptions:

$$t = \frac{r_s\sqrt{n-2}}{\sqrt{1-r_s^2}}$$

This fact allows us to adopt the t-test using the null hypothesis of no correlation between X_is and Y_is. The P-value is then computed from the t-value. The P-value is the

probability of the null hypothesis, which quantifies how rare the obtained r_s is under the null hypothesis. Stronger correlations yield a smaller P, and vice versa.

The Spearman rank correlation coefficients for proton concentrations, DOC, and EC were obtained in a similar manner.